

Supporting Information for

Fringe-controlled natural attenuation of phenoxy acids in a landfill plume: Integration of field-scale processes by reactive transport modeling

Henning Prommer^{1,}, Nina Tuxen², and Poul L. Bjerg²*

¹CSIRO Land and Water, Private Bag No. 5, Wembley WA 6913, Australia

²Institute of Environment & Resources, Technical University of Denmark

Email: *Henning.Prommer@csiro.au*; *nit@er.dtu.dk*; *plb@dtu.er.dk*

*Corresponding author phone: +61-8-93336272; fax: +61-8-9333 6211; email:
Henning.Prommer@csiro.au

This part of the Online Supporting Information contains 13 pages, including 6 Figures and 4 Tables.

3D flow and nonreactive transport model setup and calibration. The horizontal extent of the model domain was defined by (i) a no-flow boundary defined by the groundwater divide (ii) two no-flow boundaries parallel to the groundwater flow direction deduced from piezometer measurements and (iii) a fixed head boundary perpendicular to streamlines at the downstream end of the model. The vertical extent of the final flow and transport models was limited to the upper sand aquifer, after initial model runs suggested that the aquitard would act as an efficient hydraulic barrier between the upper and the lower aquifer. The position of the aquifer bottom was approximated from interpolation of discrete values that were extracted from 21 borehole logs. An initial hydraulic conductivity distribution was generated using the results from the slug tests carried out during the initial site characterization (5). The flow model was set up as a steady state model. In the absence of any influxes through horizontal model boundaries the groundwater flow in the model domain is completely driven by groundwater recharge.

Initial flow model calibration for hydraulic conductivity and groundwater recharge rate was carried out partially by manual and partially through automatic calibration by the parameter estimation tool PEST (*SI-1*) using 33 piezometric heads measurements (from within the model area) as constraints. The estimated average annual groundwater recharge of 269 mm/year was within the range of the value previously reported by Tuxen et al. (5). Following the initial flow model calibration chloride transport was simulated and compared with (i) the observations from monitoring boreholes that were screened at two different depth levels, and (ii) detailed chloride and bromide concentration profiles obtained from high resolution multi-level sampling.

The calibrated flow and nonreactive mass transport model was largely capable of matching the concentration data for chloride and bromide as well as the measured hydraulic heads (see Figure SI-1 for a comparison of simulated and measured hydraulic heads). One of the major difficulties in reproducing the field observations was the simulation of the leachate plume's apparent downward

movement between the source zone and the observation wells 100m downstream of this zone. The measured chloride concentration profiles from the MLS B1 and B2 suggested the plume's centre to be positioned very close to the bottom of the upper part of the sedimentary aquifer. Various conceptual models that could potentially explain this behaviour were tested as part of the model development and calibration process. It was explored whether (i) significant downward leakage through the clay-layer (ii) density effects (iii) a much higher permeability of the lower part of the aquifer, or (iv) uncertainty of the bore-log data interpretation could be responsible for the observed plume position and shape of the chloride concentration profile. The model runs carried out to explore those 4 hypotheses indicated that (iv) was the most likely explanation and it was concluded that a clay section that originally was interpreted as the top of the clay aquitard most likely was a clay lense that is underlain by another section of sedimentary material.

2-D reactive transport model setup and calibration. Based on the results of the 3-dimensional nonreactive transport model, a new, 2-dimensional and therefore computationally more efficient cross-sectional reactive transport model was constructed along a flow-path that was extracted from the 3-D model. The flow path was defined by forward (downstream) and backward (upstream) particle-tracking starting from the position of the multi level sampling device (MLS) B1. The model geometry and physical aquifer parameters such as hydraulic conductivity and dispersivity as well as the boundary conditions were transferred from the 3-D model to the cross-sectional model. A fixed grid cell size of $5\text{m} \times 0.2\text{m}$ was used to discretize the model in the longitudinal and vertical directions, respectively. The model calibration was carried out at this discretization level. For the final model runs the discretization was refined ($2.5\text{m} \times 0.1\text{m}$) to verify 2-D grid convergence. The simulated hydraulic gradients as well as the chloride profiles of the 3-D and the 2-D model were compared and found to be almost identical in both models, implying that transverse horizontal dispersion in the 3-D model had no significant effect on the concentration profiles at the MLS. In the field campaign that followed the calibration of the 3-D

model a second MLS (A2) was installed on the flow-path selected for the reactive transport simulations. The hydrochemical data measured at the two MLS B1 and A2 provided the major constraints for the evaluation and improvement of the conceptual hydrochemical model and for the calibration of the reaction rate parameters. The recharge water composition that was applied outside the area occupied by the landfill was based on measured water quality data from locations unaffected by landfill leachate. The recharge water composition below the landfill was estimated from samples taken near the water table in the source zone. The water compositions used as initial and boundary conditions in the model are listed in Tables SI-1 and SI-2, respectively.

Additional Literature Cited in the SI

(SI-1) Doherty, J. PEST - Model-Independent Parameter Estimation. User's manual, Fifth Edition. Watermark Numerical Computing, Brisbane, Australia, **2002**.

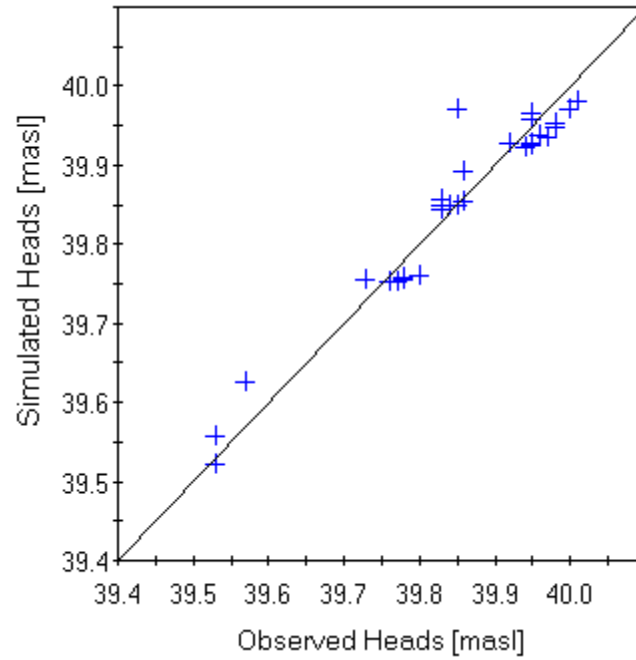


Figure SI-1. Comparison of measured hydraulic heads and heads simulated with the 3D flow model.

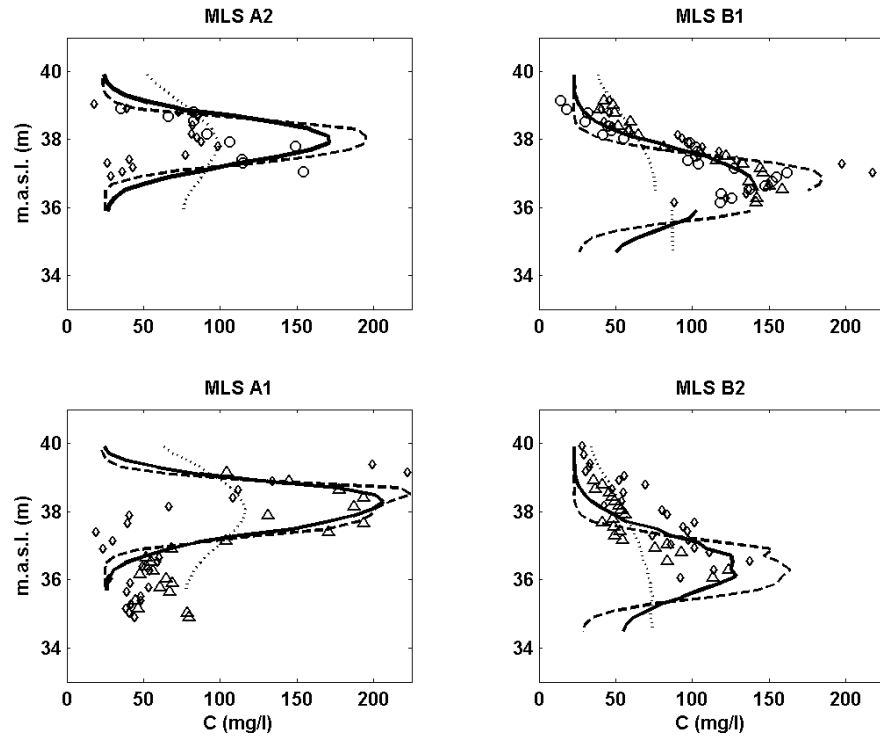


Figure SI-2. Measured and simulated (3D model) chloride concentration profiles at the four MLS A1, A2, B1 and B2: Transverse dispersivity $\alpha_T = 3\text{mm}$ (solid lines); $\alpha_T = 0.3\text{mm}$ (dotted lines); $\alpha_T = 3\text{cm}$ (dashed lines). Triangles indicate concentrations measured in September 2004, small diamonds represent measured concentrations from October 2003.

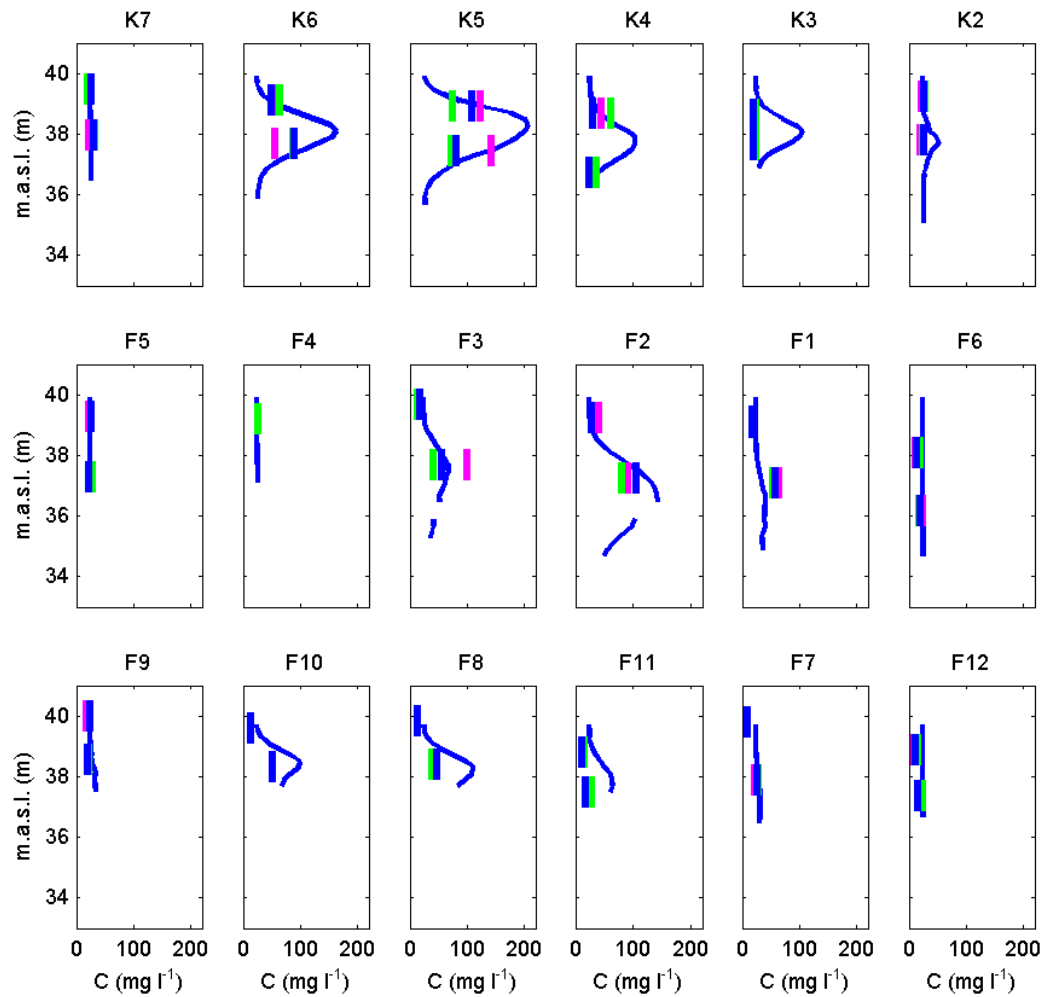


Figure SI-3. Simulated chloride concentration profiles (solid blue lines) from the 3D nonreactive transport model in comparison with measured values from the 1m-long screened monitoring wells. The measured values are plotted as bars to indicate the location of the respective well screen position and length with different colors indicating different sampling time: Blue: September 2004; Green: April 2004; Magenta: October 2003.

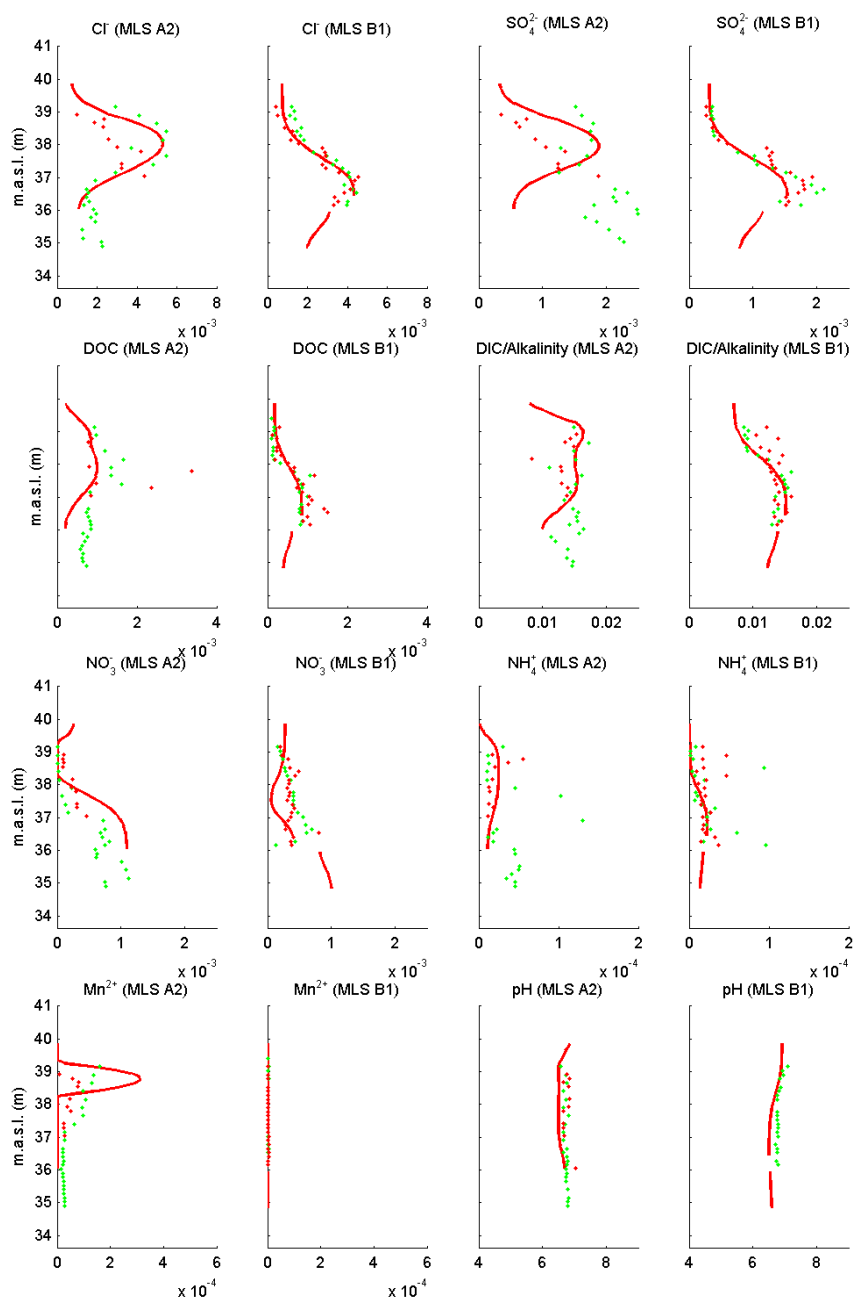


Figure SI-4. Simulated (two-dimensional model, solid red lines) and measured concentration profiles of selected aqueous components at MLS A2 and at MLS B1. Concentrations are given in mol/l (except pH). Data points in green were measured in October 2003, data points in red were measured in September 2004.

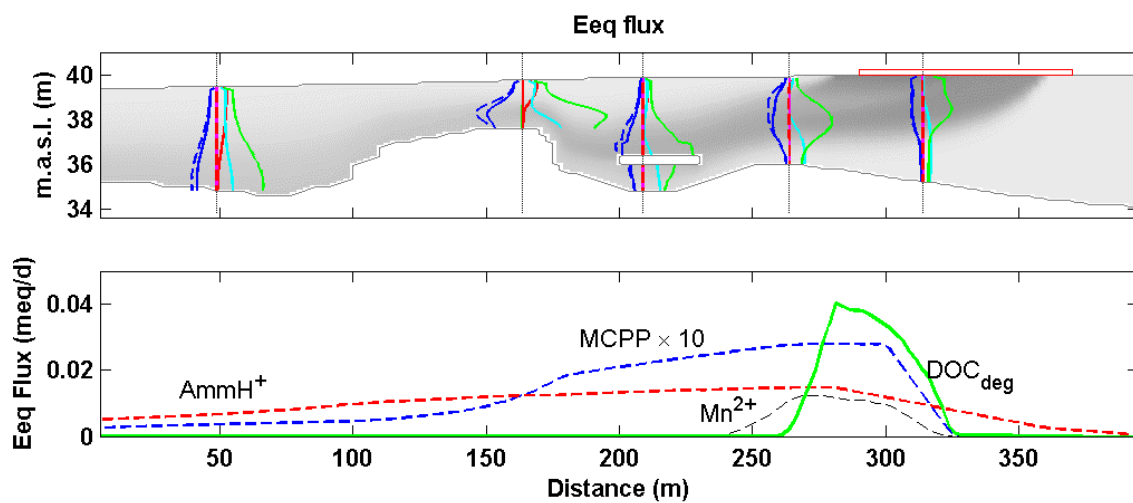


Figure SI-5. Top panel: Vertical profiles of Eeq fluxes: oxygen (red); nitrate (cyan); sulfate (green); $\text{DOC}_{\text{tot}} = \text{DOC}_{\text{deg}} + \text{DOC}_{\text{ndeg}}$ (solid blue lines); DOC_{tot} nonreactive simulation = (dashed blue line). Not visible: AmmH^+ , Mn^{2+} , MCPP, DOC_{deg} . Electron equivalents were determined from the half-reactions listed in Table SI-3. Bottom panel: Comparison of the simulated vertically integrated Eeq fluxes of AmmH^+ , DOC_{deg} , MCPP and Mn^{2+} .

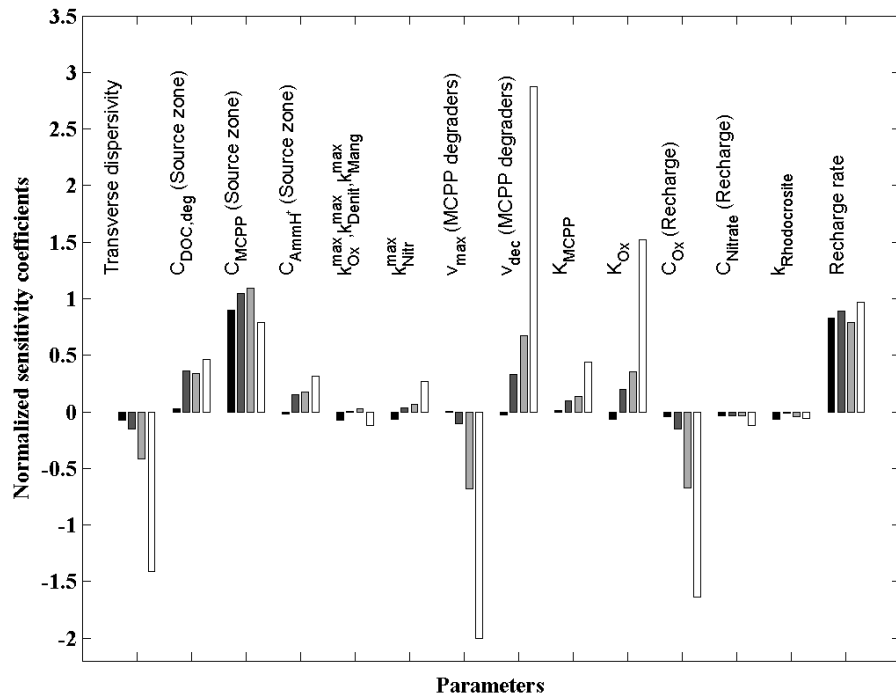


Figure SI-6. Normalised sensitivity coefficients for selected model parameters with respect to the simulated mass flux of MCPP at 4 locations: (1) near MLS A2 (darkest bars); (2) near MLS B1; (3) near Fence F and (4) near the model downstream boundary ($x = 50$ m, white bars).

Table SI-1. Modeled ambient water and recharge water composition.

Aqueous component	Ambient water composition and recharge water composition downstream/upstream of the landfill (mol l ⁻¹) ⁺⁺	Recharge water composition below landfill (mol l ⁻¹) ⁺⁺
pH	6.84	n.a.
pe	13.7	n.a.
DOC _{deg}	0	$1.0 \times 10^{-4} - 5.0 \times 10^{-4}$
DOC _{ndeg}	1.67×10^{-4}	8.00×10^{-4}
MCP	0	3.50×10^{-6}
Na	8.71×10^{-4}	3.05×10^{-3}
Cl	7.05×10^{-4}	5.65×10^{-3}
K	1.02×10^{-4}	1.54×10^{-3}
Ca	3.20×10^{-3}	7.25×10^{-3}
Mg	3.29×10^{-4}	1.32×10^{-3}
O(0)	4.00×10^{-4}	0
N(5) ⁺	$2.74 \times 10^{-4} - 1.10 \times 10^{-3}$	0
N(3) ⁺	0	3.75×10^{-5}
N(0) ⁺	0	0
Amm	0	$1.05 \times 10^{-5} - 2.50 \times 10^{-5}$
S(6) ⁺	$3.13 \times 10^{-4} - 5.31 \times 10^{-4}$	1.80×10^{-3}
S(-2) ⁺	0	0
Fe(2) ⁺	0	2.00×10^{-5}
Fe(3) ⁺	5.50×10^{-9}	0
Mn(2)	0	0
Mn(3)	0	0
C(4) ⁺	7.12×10^{-3}	1.60×10^{-2}
C(-4) ⁺	0	0

⁺Values in brackets indicate valence, ⁺⁺ except pH/pe

Table SI-2. Initial concentrations of immobile components (minerals and MCPD degraders).

Bacteria	mol l⁻¹
Aerobic MCPD degraders	1.0×10^{-10}
Minerals	mol l_b⁻¹ *
Calcite (CaCO ₃)	0.01
Goethite (FeOOH)	0.01
Pyrolusite (MnO ₂ ·H ₂ O)	0.01
Rhodochrosite (MnCO ₃)	0

* Concentrations of minerals are given as mol per litre of bulk volume

Table SI-3. Redox half-reactions used to determine the electron equivalents of the most important oxidants and reductants in the model.

Half-reaction	Electron Equivalents
$\text{O}_2 + 4 \text{H}^+ + 4 \text{e}^- \rightarrow 2 \text{H}_2\text{O}$	4
$\text{NO}_3^- + 6 \text{H}^+ + 5 \text{e}^- \rightarrow 0.5 \text{N}_2 + 3 \text{H}_2\text{O}$	5
$\text{SO}_4^{2-} + 10 \text{H}^+ + 8 \text{e}^- \rightarrow \text{H}_2\text{S} + 4 \text{H}_2\text{O}$	8
$\text{CH}_2\text{O} + 7 \text{H}^+ + 3 \text{H}_2\text{O} \rightarrow \text{HCO}_3^- + 6 \text{e}^-$	6
$\text{C}_{10}\text{H}_{11}\text{ClO}_3 + 27 \text{H}_2\text{O} \rightarrow 10 \text{HCO}_3^- + 55 \text{H}^+ + 44 \text{e}^- + \text{Cl}^-$	44
$2 \text{NH}_4^+ \rightarrow \text{N}_2 + 8 \text{H}^+ + 6 \text{e}^-$	6
$\text{NH}_4^+ + 3 \text{H}_2\text{O} \rightarrow \text{NO}_3^- + 10 \text{H}^+ + 8 \text{e}^-$	8
$\text{Mn}_2^+ + 3 \text{H}_2\text{O} \rightarrow \text{MnO}_2 \cdot \text{H}_2\text{O} + 4 \text{H}^+ + 2 \text{e}^-$	2

Table SI-4. Summary of the model discretization details and of numerical methods used.

	3-D model	2-D model
Model dimension x-direction	400 m	400 m
Minimum/Maximum discretization Δx	5 m; 10 m	2.5 m; 2.5 m
Model dimension y-direction	200 m	n.a.
Minimum/Maximum discretization Δy	5 m; 10 m	n.a.
Model dimension z-direction	7.4 m	7.4 m
Minimum/Maximum discretization Δz	0.2 m	0.1 m
Total simulation time	6000 days	6000 days
Temporal operator splitting (Transport – Reaction)	n.a.	5 days
MT3DMS advection package used	HMOC	HMOC